JOURNAL OF CHEMICAL & ENGINEERING DATA

ARTICLE

pubs.acs.org/jced

Density of Carbon Dioxide + Brine Solution from Tianjin Reservoir under Sequestration Conditions

Yi Zhang, Fei Chang,* Yongchen Song, Jiafei Zhao, Yangchun Zhan, and Weiwei Jian

Key Laboratory of the Ministry of Education of Ocean Energy Utilization and Energy Conservation, Dalian University of Technology, Dalian, Liaoning, 116024, P.R. China

ABSTRACT: Density data of carbon dioxide (CO_2) + brine solution from Tianjin reservoir were determined using magnetic suspension balance (MSB). Measurements were performed in the pressure range (10 to 18) MPa and at the temperatures (313 to 353) K. CO_2 mass fraction in solution was selected up to 0.040. The experimental results revealed that the density of CO_2 + brine solution decreases with increasing temperature and increase with increasing pressure. The density of CO_2 + brine solution increases almost linearly with increasing mass fraction of CO_2 in solution. The slope of the density vs CO_2 mass fraction curves decreased from 0.222 to 0.185 as temperature increased from 313 to 353 K and is independent of pressure. Two regression functions were developed to describe the density data of CO_2-free brine and CO_2 + brine solution from Tianjin reservoir under sequestration conditions, and the errors between experimental results and prediction were within 0.004% and 0.03%, respectively.

INSTRUCTION

The sequestration of CO_2 into geological formations (e.g., deep saline formations, depleted oil and gas fields, and unmineable coal seams), as one of carbon capture and storage (CCS) technologies, has been considered as a promising option for reducing CO_2 emissions and mitigating climate change.[1] Among all the geological formations, deep saline formations provide the largest capacity for CO_2 geological sequestration as a result of their size and wide distribution throughout the globe in all sedimentary basins. It is already known that a density difference of 0.1 $kg \cdot m^{-3}$ is sufficient to drive a natural CO_2-bearing solution to either sink or buoy,[2] which is one of the main factors affecting the safety and efficacy of CO_2 sequestration. The density value of CO_2 + brine solution is also necessary for the storage capacity estimates of the target sequestration formation. Therefore, density change of the brine due to dissolution of CO_2 under sequestration conditions is indispensable for accurate simulation of CO_2 sequestration process and CO_2 migration in formation brine.

During the last several decades, many investigators have studied the densities of aqueous CO_2 solution under deep ocean conditions such as the CO_2 seawater solution at 276.15 K and 35 MPa by Ohsumi et al.,[3] the CO_2 aqueous solution from (278.15 to 293.15) K and (6.44 to 29.49) MPa by Teng and Yamasaki.[4] Parkinson and Nevers[5] have reported the densities of CO_2 + water solution in a temperature range from (278.10 to 313.70) K and pressures up to 3.4 MPa. Yaginuma et al.[6] have measured the densities of CO_2 + distilled water solution at 304.15 K and pressures up to 10 MPa. However, these results are not suitable for CO_2 deep saline formation sequestration because of the low temperature or the low pressure. Li et al.[7] have reported the densities of CO_2 + brine solution from the Weyburn reservoir at a temperature of 332.15 K and pressures up to 29 MPa. But they have not clarified the relationship between densities of CO_2 formation brine solution and temperature. Besides, according to the analysis of Duan et al.[8] and Hu et al.,[9] most of the density data are inconsistent with each other and the accuracy is not sufficient for assessing CO_2 sequestration. In conclusion, for the density of CO_2 + brine solution under practical sequestration conditions (high pressure, elevated temperature, and various CO_2 mass fractions), more experimental measurements are required.

Table 1. Analysis of Brine Sample from Tianjin Reservoir

calcium/($mol \cdot kg^{-1}$)	0.000045
sodium/($mol \cdot kg^{-1}$)	0.020025
magnesium/($mol \cdot kg^{-1}$)	0.000143
potassium/($mol \cdot kg^{-1}$)	0.000410
iron/($mol \cdot kg^{-1}$)	0.000004
chloride/($mol \cdot kg^{-1}$)	0.012667
sulfate/($mol \cdot kg^{-1}$)	0.002094
bicarbonate/($mol \cdot kg^{-1}$)	0.001967
pH at 290.55 K	8.44

In recent years, the Chinese government has planned to launch a CO_2 sequestration pilot project in Tianjin city, located in the northeast of the North China Plain. Therefore, the present paper reports the experimental densities of CO_2 + brine solution from Tianjin reservoir. The experiments have been conducted in the pressure range (10 to 18) MPa and at temperatures (313 to 353) K. These pressure and temperature conditions were chosen on the basis of the common $p-T$ ranges ($p > 10$ MPa, $T > 313$ K) of CO_2 storage sites. In view of the solubility of CO_2 in water,[10−12] the CO_2 mass fraction in solution was selected up to 0.040. Two new equations for quantitative estimation of the densities of CO_2-free brine and CO_2 + brine solution from Tianjin reservoir under sequestration conditions have been proposed.

Received: November 11, 2010
Accepted: February 1, 2011
Published: February 22, 2011

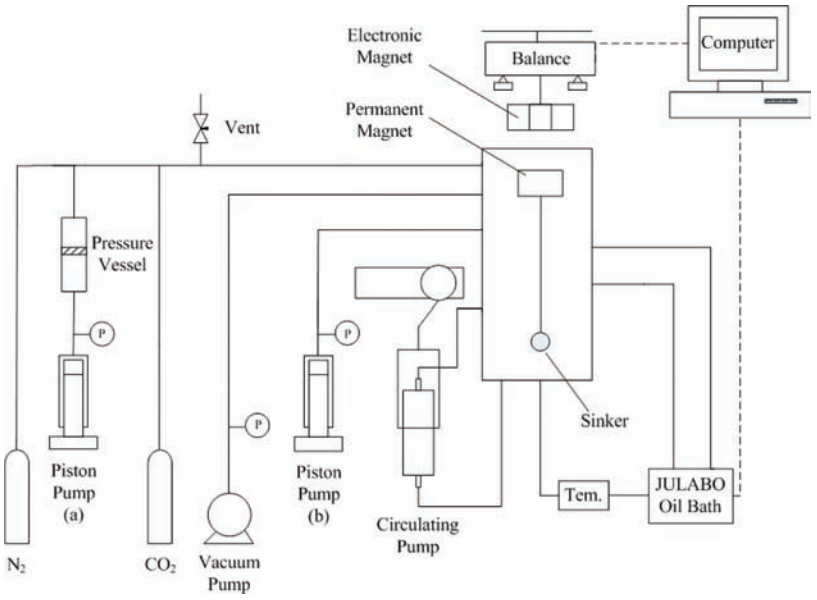

Figure 1. Schematic diagram of experimental apparatus.

Table 2. Experimental Densities ρ of CO_2-Free Brine from Tianjin Reservoir and Deviations from the Values ρ_{EOS} Calculated from EOS of Zhenhao Duan et al.[8]

T/K	st dev(T)/mK	p/MPa	st dev(p)/ kPa	ρ/g·cm^{-3}	ρ_{EOS}/g·cm^{-3}	$100\cdot(\rho - \rho_{EOS})/\rho$
313.21	6.241	10.00	0.955	0.99815	0.99776	0.039
313.24	7.790	12.01	1.018	0.99900	0.99861	0.039
313.21	7.614	14.00	0.900	0.99988	0.99947	0.041
313.17	12.151	16.01	1.227	1.00073	1.00033	0.040
313.08	4.484	18.01	0.974	1.00162	1.00121	0.041
323.20	6.370	10.01	0.932	0.99398	0.99354	0.044
323.20	11.421	12.00	0.833	0.99483	0.99438	0.045
323.22	9.546	14.01	0.509	0.99568	0.99522	0.046
323.23	13.015	16.00	0.717	0.99652	0.99606	0.046
323.21	13.160	18.01	0.659	0.99737	0.99691	0.046
332.95	9.315	10.02	1.060	0.98933	0.98883	0.051
332.97	7.940	12.01	1.129	0.99018	0.98966	0.053
332.99	8.297	14.00	0.900	0.99102	0.99050	0.052
333.00	5.931	16.00	0.422	0.99186	0.99134	0.052
333.00	5.647	18.01	0.509	0.99270	0.99218	0.052
343.00	16.918	10.00	0.830	0.98391	0.98341	0.051
343.11	21.042	12.01	0.978	0.98471	0.98421	0.051
343.20	16.918	14.01	0.999	0.98550	0.98501	0.050
343.23	15.511	16.00	0.978	0.98635	0.98584	0.052
343.22	15.036	18.01	0.797	0.98721	0.98669	0.053
353.22	16.806	10.00	0.897	0.97784	0.97737	0.048
353.11	14.540	12.01	0.999	0.97881	0.97831	0.051
353.10	11.293	14.01	1.285	0.97967	0.97918	0.050
353.12	10.826	16.00	1.139	0.98052	0.98003	0.050
353.16	9.771	18.01	0.702	0.98136	0.98087	0.050

EXPERIMENTAL SECTION

Materials. The CO_2 and N_2 were supplied by Dalian Da-te Gas Ltd. According to the gas chromatographic analysis and the dew point analysis, the purity of CO_2 and N_2 are 0.9999 and 0.99999, respectively. Both of them were used for density measurement without further purification. The brine sample belongs to the bottomhole sample. It was collected at the wellhead of the well, through which the formation brine was extracted. The Tianjin Formation is a 23−69 m thick massive sandstone formation located at a depth of 1480−1653 m beneath the ground surface. The composition of the formation brine

Table 3. Experimental Densities ρ of CO_2 + Brine Solution from Tianjin Reservoir and Deviations from the Values ρ_{EOS} Calculated from EOS of Zhenhao Duan et al.[8]

T/K	st dev(T)/mK	p/MPa	st dev(p)/kPa	ρ/g·cm^{-3}	ρ_{EOS}/g·cm^{-3}	$100\cdot(\rho - \rho_{EOS})/\rho$
			$w = 0.010$			
313.24	9.546	10.00	1.062	1.00062	1.00000	0.062
313.25	14.405	12.01	1.125	1.00148	1.00086	0.062
313.25	14.836	14.00	1.367	1.00233	1.00172	0.061
313.24	9.743	16.00	1.408	1.00317	1.00258	0.059
313.24	9.546	18.00	6.038	1.00402	1.00343	0.059
323.22	6.079	10.01	0.532	0.99645	0.99557	0.088
323.24	11.726	12.00	1.021	0.99729	0.99642	0.087
323.21	10.180	14.00	0.881	0.99815	0.99729	0.086
323.21	5.647	16.01	0.637	0.99900	0.99815	0.085
323.23	5.149	18.00	0.798	0.99983	0.99898	0.085
333.22	7.638	10.19	0.539	0.99167	0.99061	0.107
333.24	5.686	12.00	0.700	0.99244	0.99138	0.107
333.24	7.020	14.00	0.780	0.99329	0.99224	0.106
333.22	10.376	16.00	0.408	0.99414	0.99310	0.105
333.19	6.000	18.00	0.957	0.99501	0.99397	0.105
343.23	9.634	10.01	2.955	0.98620	0.98495	0.127
343.21	5.836	12.01	1.180	0.98706	0.98583	0.125
343.18	4.702	14.00	0.999	0.98794	0.98671	0.125
343.18	6.757	16.00	0.717	0.98879	0.98758	0.122
343.17	5.898	18.01	0.884	0.98965	0.98844	0.122
353.25	15.718	10.00	7.743	0.98017	0.97887	0.133
353.23	14.127	12.00	7.013	0.98105	0.97976	0.131
353.22	14.136	14.00	4.180	0.98193	0.98065	0.130
353.20	10.360	16.01	0.926	0.98283	0.98154	0.131
353.18	6.761	18.00	1.239	0.98370	0.98242	0.130
			$w = 0.021$			
313.13	5.936	10.01	0.884	1.00311	1.00252	0.059
313.16	4.523	12.01	1.267	1.00396	1.00338	0.058
313.14	6.216	14.01	1.168	1.00482	1.00426	0.056
313.14	9.962	16.00	1.311	1.00566	1.00512	0.054
313.15	10.553	18.00	1.165	1.00650	1.00598	0.052
323.13	18.173	10.01	1.032	0.99881	0.99786	0.095
323.09	2.887	12.01	0.669	0.99968	0.99875	0.093
323.12	4.924	14.01	0.793	1.00053	0.99961	0.092
323.12	9.002	16.00	0.902	1.00135	1.00047	0.088
323.14	8.065	18.01	1.215	1.00217	1.00132	0.085
333.15	13.126	10.01	0.859	0.99387	0.99259	0.129
333.14	11.389	12.01	1.007	0.99472	0.99347	0.126
333.14	12.496	14.02	0.834	0.99558	0.99435	0.124
333.13	8.732	16.01	1.493	0.99643	0.99522	0.121
333.13	7.267	18.00	0.959	0.99727	0.99608	0.119
343.15	5.774	10.01	0.645	0.98833	0.98682	0.153
343.14	6.903	12.01	1.007	0.98920	0.98771	0.151
343.14	8.681	14.02	0.884	0.99006	0.98860	0.147
343.13	8.242	16.01	0.881	0.99091	0.98947	0.145
343.13	13.290	18.00	1.251	0.99176	0.99034	0.143
353.15	14.528	10.01	1.308	0.98217	0.98059	0.161
353.16	7.614	12.01	1.532	0.98302	0.98148	0.157
353.17	14.689	14.02	0.676	0.98391	0.98237	0.157
353.13	16.129	16.02	0.722	0.98479	0.98329	0.152
353.10	8.836	18.02	0.999	0.98567	0.98419	0.150

dx.doi.org/10.1021/je101214e |J. Chem. Eng. Data 2011, 56, 565–573

Table 3. Continued

T/K	st dev(T)/mK	p/MPa	st dev(p)/kPa	ρ/g·cm^{-3}	ρ_{EOS}/g·cm^{-3}	$100\cdot(\rho - \rho_{EOS})/\rho$
			w = 0.030			
313.09	5.964	10.02	1.718	1.00489	1.00458	0.031
313.08	9.931	12.01	0.402	1.00574	1.00547	0.027
313.05	9.409	14.01	1.032	1.00660	1.00636	0.024
313.06	6.806	16.01	0.745	1.00744	1.00723	0.021
313.07	9.079	18.00	0.690	1.00828	1.00809	0.019
323.07	11.055	10.00	1.376	1.00053	0.99975	0.078
323.07	14.225	12.01	0.501	1.00138	1.00063	0.075
323.07	10.646	14.01	0.403	1.00223	1.00151	0.072
323.07	13.585	16.01	1.200	1.00308	1.00238	0.070
323.05	10.029	18.01	0.745	1.00392	1.00325	0.067
333.06	5.936	10.04	4.096	0.99548	0.99433	0.116
333.07	9.759	12.01	0.816	0.99632	0.99520	0.112
333.06	5.964	14.02	1.020	0.99719	0.99609	0.110
333.04	11.293	16.01	0.999	0.99804	0.99698	0.106
333.02	8.847	18.01	0.475	0.99889	0.99787	0.102
343.08	13.667	10.01	0.917	0.98981	0.98838	0.144
343.07	13.825	12.01	0.875	0.99068	0.98928	0.141
343.02	8.837	14.01	0.915	0.99155	0.99021	0.135
343.03	10.072	16.01	0.824	0.99241	0.99109	0.133
343.08	5.936	18.01	1.187	0.99325	0.99194	0.132
353.07	12.459	10.00	0.516	0.98366	0.98202	0.167
353.09	15.607	12.01	1.291	0.98455	0.98292	0.166
353.06	10.744	14.01	0.556	0.98544	0.98384	0.162
353.07	16.918	16.01	0.721	0.98624	0.98473	0.153
353.07	12.836	18.00	0.632	0.98709	0.98562	0.149
			w = 0.040			
313.04	12.158	10.01	0.717	1.00711	1.00690	0.021
313.07	14.346	12.01	0.929	1.00795	1.00777	0.018
313.07	13.933	14.02	1.160	1.00880	1.00866	0.014
313.06	7.838	16.01	0.680	1.00964	1.00955	0.009
313.05	11.100	18.01	0.832	1.01048	1.01043	0.005
323.03	15.299	10.01	1.083	1.00262	1.00185	0.077
322.99	8.729	12.01	1.670	1.00349	1.00276	0.073
323.05	13.529	14.01	1.049	1.00432	1.00361	0.071
323.11	5.145	16.01	1.200	1.00513	1.00447	0.066
323.10	3.755	18.00	1.235	1.00597	1.00535	0.062
333.06	7.614	10.02	1.579	0.99746	0.99619	0.127
333.07	6.594	12.01	0.900	0.99832	0.99708	0.124
333.06	5.500	14.02	1.141	0.99917	0.99799	0.118
333.06	5.036	16.01	0.977	1.00002	0.99888	0.114
333.06	5.090	18.00	0.992	1.00087	0.99976	0.111
343.06	13.229	12.01	1.938	0.99255	0.99099	0.157
343.13	14.039	14.02	0.565	0.99338	0.99186	0.153
343.07	15.581	16.02	0.917	0.99429	0.99279	0.151
343.03	12.623	18.00	0.759	0.99516	0.99371	0.146
353.07	5.898	14.01	1.276	0.98707	0.98540	0.169
353.05	14.346	16.02	1.248	0.98797	0.98632	0.167
353.02	5.903	18.00	1.102	0.98887	0.98724	0.165

sample was determined and the results were presented in Table 1. The cations in the sample were determined using atomic absorption spectrophotometer with flame atomization (Unicam model 969). The anions in the sample were determined by ion-chromatography (Shimadzu SCL-10A$_{SP}$) with nonsuppressor conductivity detector.

Apparatus. The experimental apparatus is shown schematically in Figure 1. The main apparatus was the MSB, including a

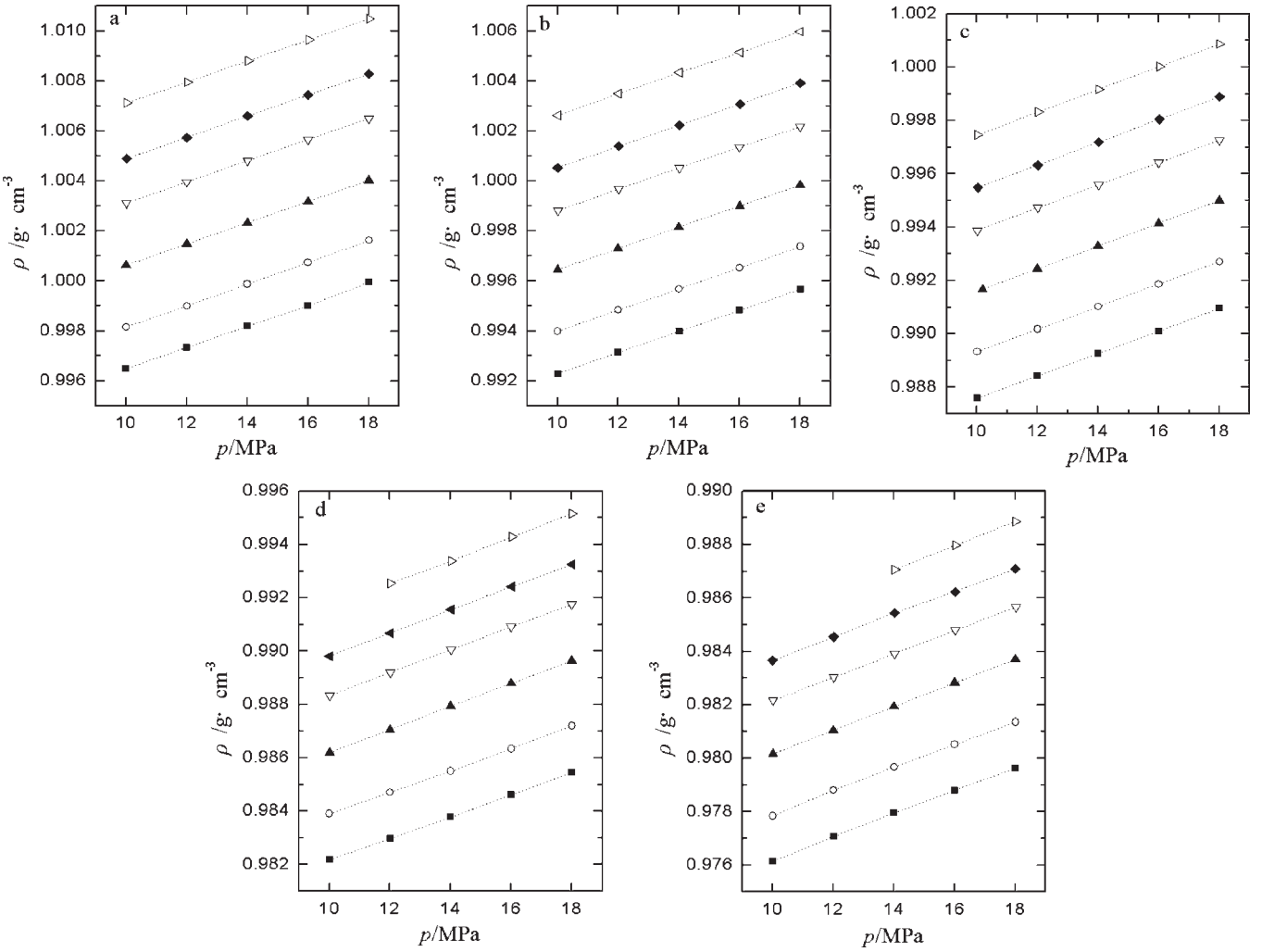

Figure 2. Density of CO_2-free brine and CO_2 + brine solution from Tianjin reservoir versus pressure p/MPa at different temperatures and CO_2 concentrations: a, 313 K; b, 323 K; c, 333 K; d, 343 K; e, 353 K; ■, pure water; ○, CO_2-free brine; ▲, $w = 0.010$; ▽, $w = 0.021$; ◆, $w = 0.030$; △, $w = 0.040$; dots: experimental; Line: predicted.

microbalance, a measuring cell, a sinker, a magnetic suspension coupling, and a control system, manufactured by Rubotherm Präzisionsmesstechnik GmbH. The MSB installed in our laboratory was suitable for operation in the temperature range (253 to 423) K and at pressures up to 20 MPa. The temperature in density measurement was controlled with a double-walled thermostatic jacket, which fits exactly around the measuring cell. The jacket was filled with circulating oil, whose temperature was controlled with a JULABO FP 50-ME Refrigerated/Heating Circulator. The sample temperature was measured with a Pt100 temperature probe located in the measuring cell just below the sinker. The controlling accuracy of temperature was ±0.01 K. The pressure was measured with a pressure sensor (20 MPa, reproducibility 0.08%) located in a measuring gas connection tube by means of a T-piece. To enhance the dissolution of CO_2 and maintain CO_2 solution inside the measuring cell in a uniform state, a circulating pump (AKICO, Japan) was installed. The piston pump (a) and the pressure vessel were used to pressurize the nitrogen to the exact pressure in leakage detection of the experimental system. The piston pump (b) was used to pressurize and transfer the brine sample.

Before the experiment, the densities of nitrogen and deionized water were measured to test the accuracy and reliability of the experimental system. Nitrogen and deionized water were chosen to be test fluids mainly because their densities have been studied extensively. Comparison of experimental results and the standard values taken from National Institute of Standards and Technology (NIST) shows that our experiment values are in good accordance with the standard values with a maximum deviation of 0.05% for N_2 and 0.03% for water within the temperature and pressure range studied.

Principle of Operation. The working principle of the MSB has been described extensively elsewhere.[13,14] Nevertheless, several important points should be noted here. The main advantage of MSB compared with other densimeters is that the magnetic suspension coupling allows the measuring force to be transmitted contactlessly from the measuring cell to a microbalance at ambient atmosphere. This means that mass changes of a sample can be recorded even under extreme conditions with the utmost accuracy.

For a MSB, the buoyancy method using Archimedes' principle is used to obtain high precision density measurements by a sinker, whose volume is known, weighed in a measuring fluid. The buoyancy that the sinker experiences indicates the density of

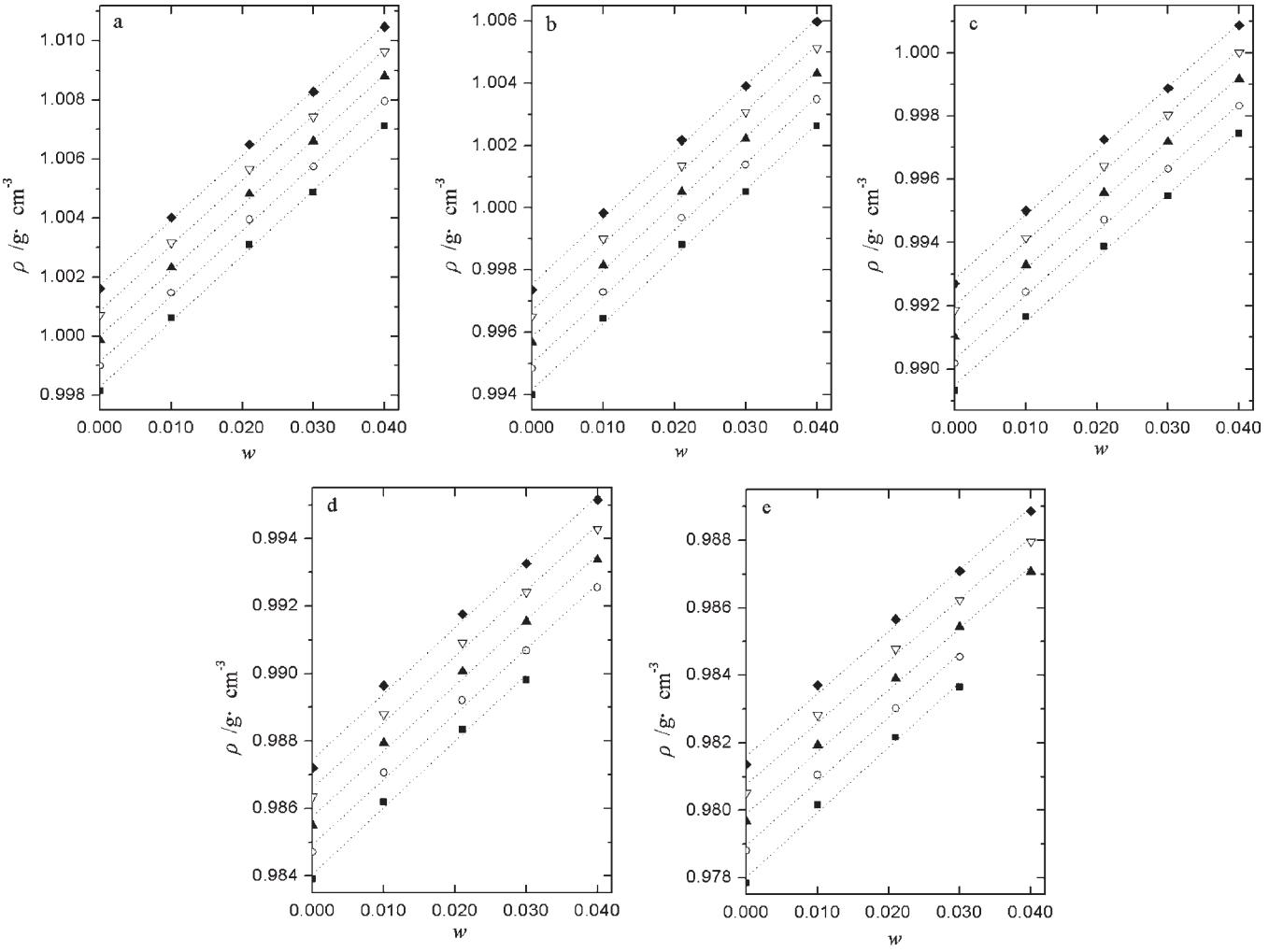

Figure 3. Density of CO_2 + brine solution from Tianjin reservoir versus CO_2 mass fraction under selected pressures at different temperatures: a, 313 K; b, 323 K; c, 333 K; d, 343 K; e, 353 K; ■, 10 MPa, ○, 12 MPa, ▲, 14 MPa, ▽, 16 MPa, ◆, 18 MPa; dots, experimental; line, predicted.

the fluid. According to Archimedes' principle, the density of the measured fluid can be calculated from

$$\rho = \frac{m - W}{V} \tag{1}$$

where m is the true (vacuum) mass of the sinker; W is its apparent mass (weighed in fluid-filled measuring cell); and V is the volume of the sinker at absolute temperature T and pressure p, which can be obtained accurately from its known volume, V_0, at specified reference conditions (T_0, p_0) from the expression:

$$V = V_0\left[1 + \alpha_T(T - T_0) - \frac{1}{K_T}(p - p_0)\right] \tag{2}$$

where α_T is the isobaric thermal expansion coefficient and K_T is the isothermal compressibility module. Both of α_T and K_T are functions of temperature for the sinker material and were informed by the manufacturer of the MSB.

■ RESULTS AND DISCUSSION

Experimental Densities. The measured densities of CO_2-free brine and CO_2 + brine solution from Tianjin reservoir are presented in Tables 2 and 3, respectively. Each data point represents the average result from ten measurements or more. The uncertainty of CO_2-free brine density caused by pressure and temperature measurement is assessed to be 0.01% and that of CO_2 + brine solution density results from pressure and temperature measurement, as well as CO_2 mass fraction analysis, is estimated to be 0.025%. The uncertainty caused by sinker volume determination, force transmission error, and balance weightings are included in the total uncertainty of the MSB. The total uncertainty of the MSB is 0.1% as stated in the technical specification.

The experimental values are compared to the values calculated for the EOS proposed by Zhenhao Duan et al.[8] As shown in Table 2, the experimental densities of CO_2-free brine agree with the calculated values within 0.053%. Table 3 shows that the experimental densities of the CO_2 + brine solution and the calculated values are also consistent with each other within 0.17%, with an average relative deviation of about 0.1%.

These experimental results are also plotted as a function of pressure for different CO_2 concentrations at different temperatures in Figure 2. The solid rectangles and the open circles represent the density of pure water taken from NIST and the experimental density of CO_2-free brine, respectively. The rest of the plots represent the densities of CO_2 + brine solution at

dx.doi.org/10.1021/je101214e |J. Chem. Eng. Data 2011, 56, 565–573

Table 4. Coefficients in eqs 3 and 4

i	a_i	b_i	c_i	d_i	e_i
0	8.11951×10^{-1}	1.83484×10^{-3}	8.255116×10^{-1}	6.453167×10^{-4}	3.300099×10^{-3}
1	1.54810×10^{-3}	-8.65129×10^{-6}	1.463710×10^{-3}	-1.401649×10^{-6}	1.380885×10^{-6}
2	-3.08794×10^{-6}	1.32615×10^{-8}	-2.954866×10^{-6}	2.218350×10^{-9}	-1.567212×10^{-8}

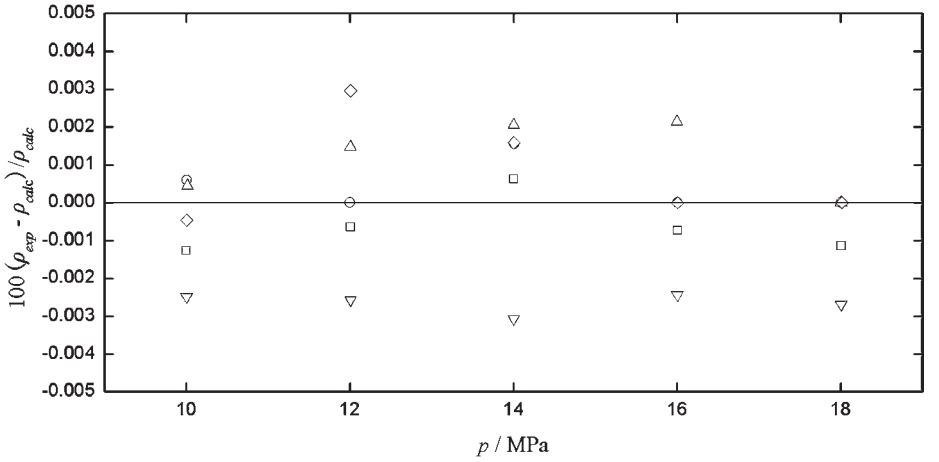

Figure 4. Deviations of experimental densities ρ_{exp} of CO_2-free brine from the correlation of eq 3 ρ_{calc} versus pressure p/MPa at different temperatures: □, 313 K; ○, 323 K; △, 333 K; ▽, 343 K; ◇, 353 K.

different CO_2 concentrations, w. As shown in Figure 2, the density of Tianjin brine is larger than that of pure water at the same experimental conditions. For a given CO_2 mass fraction, the density of CO_2 + brine solution increases with increasing pressure almost linearly. The slopes of the solution density curves appeared to be the same as that of the CO_2-free brine and pure water within experimental error.

The measured results are also plotted as a function of CO_2 mass fraction for different pressures at different temperatures in Figure 3. In Figure 3, the intercept of each curve represents the density of the CO_2-free brine. As shown in Figure 3, for a constant pressure, the density of CO_2 brine solution increased with increasing CO_2 mass fraction almost linearly. Haugen et al.[2] and Song et al.[15] explained this phenomenon before. They claimed that the slopes of the CO_2 seawater solution density vs CO_2 mass fraction curves were 0.182 and 0.275 $g \cdot cm^{-3}$, respectively, and were independent of temperature. However, according to our research, the slope of the CO_2 brine solution density vs CO_2 mass fraction curves is closely related to temperature; it decreases from 0.222 to 0.185 $g \cdot cm^{-3}$ as the temperature increases from 313 to 353 K. This trend is conceivable because according to Lu et al.,[16] the density of CO_2 brine solution can be less than that of the surrounding CO_2-free formation brine when the temperature is higher than the equal density temperature (varying with pressure and salinity of the formation brine). In this case, the plume of dissolved CO_2 will mitigate upward due to buoyancy force and leak to groundwater aquifers or to the surface. In other words, formations with higher temperatures are less suitable for CO_2 storage than cooler formations, if all other conditions remain unchanged.

And it also can be found from the Figure 3 that the slope of the CO_2 + brine solution density vs CO_2 mass fraction curves is independent of pressure, which is in accordance with the existing results.[3,7]

Fitting of the Experimental Density Data. The density of CO_2-free brine is a function of both temperature and pressure. As Figure 2 shows, it is proportional to pressure at a constant temperature. On the basis of this relationship, the experimental density data of CO_2-free brine have been fitted to an equation:

$$\rho_0/(g \cdot cm^{-3}) = \sum_{i=0}^{2} (a_i + b_i p/\mathrm{MPa})(T/\mathrm{K})^i \qquad (3)$$

where T is temperature, p is pressure; a_i and b_i are coefficients and are presented in Table 4.

The density of CO_2 + brine solution is a function of temperature, pressure and CO_2 mass fraction. As shown in Figures 2 and 3, it is proportional to pressure and CO_2 mass fraction. The experimental data of CO_2 brine solution have also been fitted to an equation:

$$\rho/(g \cdot cm^{-3}) = \sum_{i=0}^{2} (c_i + d_i p/\mathrm{MPa} + e_i w')(T/\mathrm{K})^i \qquad (4)$$

where T is temperature; p is pressure; w is the mass fraction of CO_2 in the solution; w' is the CO_2 mass percentage, $w' = w \times 100$; c_i, d_i, e_i are coefficients that can be estimated by minimizing the residual sum of squares. The results are presented in Table 4.

The functional form of eqs 3 and 4 was chosen on the basis of giving the smallest residuals for interpolation over the experimental conditions. Moreover, these equations enable the data to be cast into isothermal or isobaric forms to facilitate comparison with other experimental data.

For the five isotherms and the pressure range we have explored, Figure 4 shows the relative deviation of each experimental density value of CO_2-free brine from the value calculated from eq 3 as a function of pressure. As can be seen, eq 3 can accurately reproduce the experimental data, where the average deviation is 0.002% and the maximum deviation is 0.004%.

dx.doi.org/10.1021/je101214e |J. Chem. Eng. Data 2011, 56, 565–573

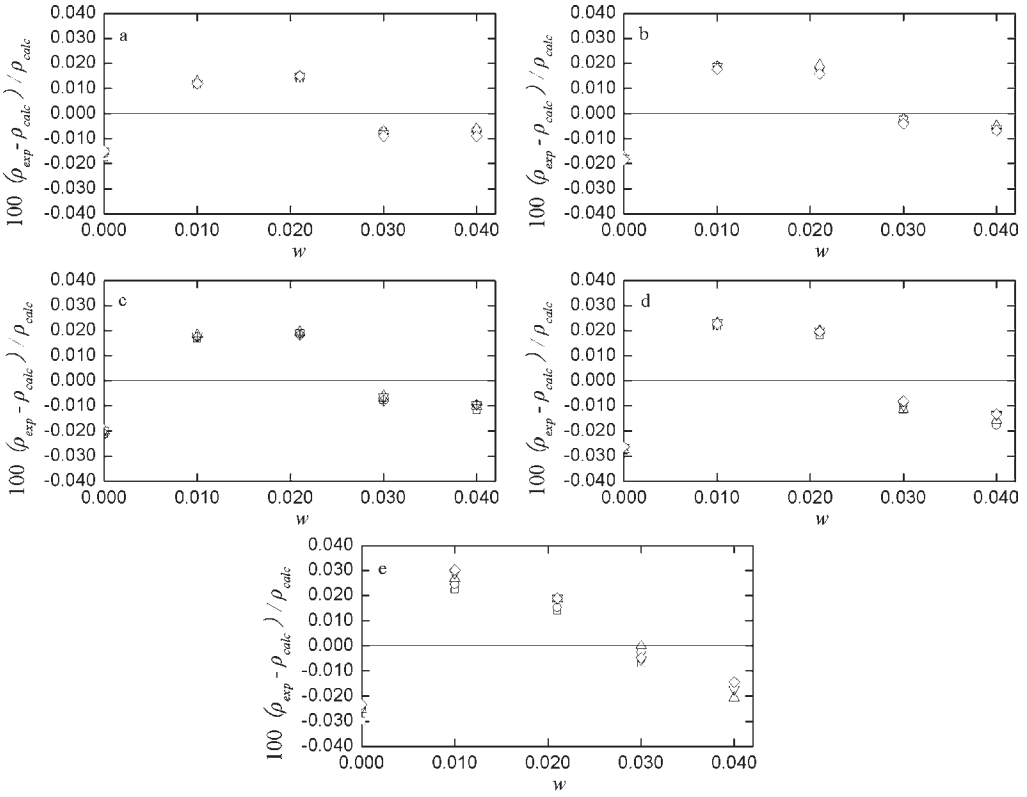

Figure 5. Deviations of experimental densities ρ_{exp} of CO_2 + brine solutions from the correlation of eq 4 ρ_{calc} versus CO_2 mass fraction under selected pressures at different temperatures: a, 313 K; b, 323 K; c, 333 K; d, 343 K; e, 353 K; □, 10 MPa, ○, 12 MPa, △, 14 MPa, ▽, 16 MPa, ◇, 18 MPa.

Figure 5 shows the relative deviation of experimental density value of CO_2 + brine solution from the value calculated from eq 4 as a function of CO_2 mass fraction at different temperatures. Comparing the experimental values and the calculated values, the (p, ρ, T, w) surfaces defined by eq 4 with the parameters listed in Table 4 describe the whole set of the present experimental results with maximum deviation of 0.03%, across the temperature range from (313 to 353) K and at pressures up to 18 MPa, which indicates that eq 4 can correlate the density data of CO_2 + brine solution from Tianjin reservoir well.

CONCLUSIONS

In this work, we studied the influence of the pressure [(10, 12, 14, 16, 18) MPa], the temperature [(313, 323, 333, 343, 353) K], and the concentration of CO_2 [(0.010, 0.021, 0.030, 0.040) mass fraction] on the density of Tianjin formation brine. The following conclusions were obtained: (1) Dissolution of CO_2 increases the densities of CO_2 Tianjin formation brine. (2) For a constant CO_2 mass fraction, the density of CO_2 brine solution increases linearly with increasing pressure. (3) For a constant pressure, the density of CO_2 brine solution increases linearly with increasing CO_2 mass fraction in solution. The slope of the density vs CO_2 mass fraction decreases from 0.222 to 0.185 as the temperature increased from 313 to 353 K and is independent of pressure. (4) The prediction gave a good fit to the experimental density data of CO_2-free brine and CO_2 + brine solution.

AUTHOR INFORMATION

Corresponding Author

*E-mail: f_chang@foxmail.com.

Funding Sources

This work was supported by the National High Technology Research and Development Program of China (863 Program) (No. 2008AA062303 and No. 2009AA063402) and the State Key Program of National Natural Science of China (No. 50736001). We also thank the Fundamental Research Funds for the Central Universities and National Natural Science Foundation of China (No. 51006016, No. 51006017).

ACKNOWLEDGMENT

We thank the editor for his kind work and are grateful for the constructive comments from the reviewers.

REFERENCES

(1) Anderson, S.; Newell, R. Prospects for carbon capture and storage technologies. *Annu. Rev. Environ. Resour.* **2004**, *29*, 109–42.

(2) Drange, H.; Haugan, P. M. Carbon-dioxide sequestration in the ocean - the possibility of injection in shallow-water. *Energy Convers. Manage.* **1992**, *33*, 697–704.

(3) Ohsumi, T.; Nakashiki, N.; Shitashima, K.; Hirama, K. Density change of water due to dissolution of carbon dioxide and near- field behavior of CO_2 from a source on deep-sea floor. *Energy Convers. Manage.* **1992**, *33*, 685–690.

(4) Teng, H.; Yamasaki, A.; Chun, M.-K.; Lee, H. Solubility of liquid CO_2 in water at temperatures from 278 to 293 K and pressures from 6.44 to 29.49 MPa and densities of the corresponding aqueous solution. *J. Chem. Thermodyn.* **1997**, *29*, 1301–1310.

(5) Parkinson, W. J.; Nevers, N. D. Partial molal volume of carbon dioxide in water solution. *Ind. Eng. Chem. Fundam.* **1969**, *8*, 709–713.

(6) Yaginuma, R.; Sato, Y.; Kodama, D.; Tanaka, H.; Kato, M. Saturated densities of carbon dioxide + water mixture at 304.1 K and pressures up to 10 MPa. *Nihon Enerugi Gakkaishi* **2000**, *79*, 144–146.

(7) Li, Z.; Dong, M.; Li, S.; Dai, L. Densities and solubilities for binary systems of carbon dioxide + water and carbon dioxide + brine at 59 ^{o}C and pressures to 29 MPa. *J. Chem. Eng. Data* **2004**, *49*, 1026–1031.

(8) Duan, Z.; Hu, J.; Li, D. Densities of the CO_2-H_2O and CO_2-H_2O-NaCl systems up to 647 K and 100 MPa. *Energy Fuels* **2008**, *22*, 1666–1674.

(9) Hu, J.; Duan, Z.; Zhu, C.; Chou, I. *PVTx* properties of the CO_2-H_2O and CO_2-H_2O-NaCl systems below 647 K: Assessment of experimental data and thermodynamic models. *Chem. Geol.* **2007**, *238*, 249–267.

(10) Bamberger, A.; Sieder, G.; Maurer, G. High-pressure (vapor + liquid) equilibrium in binary mixtures of (carbon dioxide + water or acetic acid) at temperatures from 313 to 353 K. *J. Supercrit. Fluids* **2000**, *17*, 97–110.

(11) King, M. B.; Mubarak, A.; Kim, J. D.; Bott, T. R. The Mutual Solubilities of Water with Supercritical and Liquid Carbon Dioxide. *J. Supercrit. Fluids* **1992**, *5*, 296–302.

(12) Duan, Z.; Sun, R.; Zhu, C.; Chou, I. An Improved Model for the Calculation of CO_2 Solubility in Aqueous Solutions Containing Na^+, K^+, Ca^{2+}, Cl^- and SO_4^{2-}. *Mar. Chem.* **2005**, *98*, 131–139.

(13) Wagner, W.; Brachthauser, K.; Kleinrahm, R.; Lösch, H. W. A New, Accurate single-sinker densitometer for temperatures from 233 to 523 K at pressures up to 30 MPa. *Int. J. Thermophys.* **1995**, *16*, 399–411.

(14) Wagner, W.; Kleinrahm, R. Densimeters for very accurate density measurements of fluids over large ranges of temperature, pressure, and density. *Metrologia* **2004**, *41*, S24–S39.

(15) Song, Y.; Chen, B.; Nishio, M.; Akai, M. The study on density change of carbon dioxide seawater solution at high pressure and low temperature. *Energy* **2005**, *30*, 2298–2307.

(16) Lu, C.; Han, W. S.; Lee, S. Y.; McPherson, Brian J.; Peter, C.; Lichtner Effects of density and mutual solubility of a CO_2 + brine system on CO_2 storage in geological formations: "Warm" vs. "cold" formations. *Adv. Water Resour.* **2009**, *32*, 1685–1702.